Eur. Phys. J. A **1**, 91–98 (1998)

THE EUROPEAN PHYSICAL JOURNAL A

OZI rule violation in $p\bar{p}$ annihilation into $\phi\pi\pi$ by two step processes

V.E. Markushin, M.P. Locher

Paul Scherrer Institute, CH-5232 Villigen PSI, Switzerland

Received: 4 August 1997

Abstract. The $\phi\pi^+\pi^-$ production in $p\bar{p}$ annihilation at rest is strongly enhanced by a two step mechanism with intermediate $K\bar{K}\pi\pi$ states. The relative yield of the ϕ production due to the resonant final state interaction decreases with increasing total energy of the $p\bar{p}$ system.

PACS. 13.75.Cs Nucleon-nucleon interactions – 12.40.-y Other models for strong interactions – 14.40.Cs Other mesons with S=C=O, mass < 2.5 GeV

1 Introduction

The production of ϕ mesons in low energy $p\bar{p}$ annihilation (see [1–6] and references therein) is strongly enhanced in some channels for which the ϕ production is expected to be suppressed on the tree level according to the Okubo-Zweig-Iizuka (OZI) rule [7–9]. These conspicuously OZI rule violating reactions are of considerable theoretical interest since they can be used for studying reaction mechanisms and the nucleon structure, in particular the problem of an intrinsic $s\bar{s}$ component [10–12]. Some well-known OZI-rule breaking mechanisms are two-step processes with ordinary hadrons in the intermediate state [13], therefore their role in the $p\bar{p}$ annihilation must be investigated.

The two step mechanisms in nucleon-antinucleon annihilation have been studied for various final states containing ϕ mesons [14–23]. It has been found that in the $\phi\pi$ and $\phi\phi$ channels, which show the most dramatic violation of the OZI rule, two-step mechanisms play an important role and result in a cross section comparable with the experimental data. However, for a number of reactions, including $p\bar{p} \to \phi\rho,\ \phi\pi\pi,\ \phi\omega$, no significant contributions from two-step mechanisms have been found. The goal of this paper is to reanalyze the role of two-step mechanisms for the $p\bar{p}$ annihilation into the $\phi\pi\pi$ channel. To this aim we go beyond the approximations used in previous studies. The resulting cross sections turn out to have the right order of magnitude. The plan of the paper is as follows. Sect. 2 gives a brief summary of the experimental data and the previous calculations. A simple model illustrating the two-step mechanism with a resonant final state interaction is considered in Sect. 3. The reaction $p\bar{p} \to \phi\pi\pi$ is discussed in Sect. 4 where the two-step mechanism with the $K\bar{K}\pi\pi$ intermediate state is studied in detail. The summary of the results is given in Sect. 5. For earlier reviews concerning the two-step mechanisms we refer to [24–28].

2 The OZI rule violation in $p\bar{p} \to \phi\pi^+\pi^-, \phi\rho, \phi\omega$

Table 1 gives a summary of the experimental data on the OZI rule violation in the $\phi\pi^+\pi^-$ and $\phi\rho$ channels at different energies. The tree level expectations based on the deviation of the $\omega - \phi$ mixing angle from the ideal one are $(\Theta - \Theta_i)^2 \sim 4 \cdot 10^{-3}$ [34]. The OZI rule violation in these channels is therefore rather moderate[1]. The experimental branching ratios for the reactions $p\bar{p} \to \pi\pi\phi,\ \rho\phi,\ \pi\pi\omega, \rho\omega,\ \pi\pi K\bar{K}$ at rest are given in Table 2.

Until now the importance of the two-step mechanisms in the reactions $p\bar{p} \to \phi\pi\pi$, $p\bar{p} \to \phi\rho$, $p\bar{p} \to \phi\omega$ remained unclear. The main attention was focused on two-particle intermediate states (two meson doorway approximation). The contribution of the $K^*\bar{K} + K\bar{K}^*$ intermediate state was considered in the unitarity approximation in [17]; the calculated branching ratios for the $\phi\rho$ and $\phi\omega$ channels were found to be about two orders of magnitude smaller than observed. The possibility of a large contribution of the $\rho\omega$ intermediate state for the $\phi\pi\pi$ channel was pointed out in [16], however the estimate was done in unitarity approximation and neglecting spin. Since the unitarity approximation is likely to be suppressed by threshold factors, the off-mass-shell contributions can be large, but they are also known to be model dependent. Intermediate states with more than two particles should also be taken into account.

Of special interest are the intermediate states containing $K\bar{K}$, because the $K\bar{K}$ production is not OZI suppressed and the final state interaction (FSI) effects are strong if the $K\bar{K}$ system is produced in the region of the ϕ

[1] This magnitude of the OZI rule breaking is often termed nondramatic, contrary to the cases where the ϕ production exceeds the estimate from $\phi - \omega$ mixing by more than one order of magnitude

Table 1. The relative probabilities for the $\phi\rho, \omega\rho$ and $\phi\pi^+\pi^-, \omega\pi^+\pi^-$ channels in $p\bar{p}$ annihilation *vs.* antiproton momentum. Phase space corrected ratios of yields are also tabulated

$p_{\bar{p}}$(GeV/c)	$\frac{BR(\phi\rho)}{BR(\omega\rho)} \cdot 10^3$		$\frac{BR(\phi\pi^+\pi^-)}{BR(\omega\pi^+\pi^-)} \cdot 10^3$		Ref.
	measured	PS corrected	measured	PS corrected	
0 (gas)	6.3 ± 1.6				[1,29]
0 (gas/LX)	7.5 ± 2.4				[1,29]
0 (liq.)			7.0 ± 1.4	15 ± 3	[30]
0 (liq.)			4.9 ± 0.8	10.3 ± 1.6	[6]
0 (3 atm)			5.9 ± 0.9	12.5 ± 2.0	[6]
0.76	9 ± 5	13 ± 4	10.0 ± 2.4	19 ± 5	[31]
1.2			11^{+3}_{-4}	19^{+5}_{-7}	[32]
2.3	22 ± 13	25 ± 15	21 ± 5	30 ± 7	[33]
3.6			9^{+4}_{-7}	12^{+5}_{-9}	[32]

Table 2. The experimental branching ratios for $p\bar{p}$ annihilation at rest into $\pi\pi K\bar{K}$, $\rho\phi$, and $\pi\pi\phi$

Reaction	BR	Condition	Ref.
$p\bar{p} \to \pi^+\pi^-\phi$	$4.6(9) \cdot 10^{-4}$	liq.	[30]
	$5.4(10) \cdot 10^{-4}$	gas	[1]
	$7.7(17) \cdot 10^{-4}$	gas LX	[1]
	$4.7(11) \cdot 10^{-4}$	S	[1]
	$6.6(15) \cdot 10^{-4}$	P	[1]
	$3.5(4) \cdot 10^{-4}$	liq.	[6]
	$3.7(5) \cdot 10^{-4}$	gas	[6]
$p\bar{p} \to \pi^+\pi^-\phi_{\to K_S K_L}$	$1.8(3) \cdot 10^{-4}$	liq.	[35]
$p\bar{p} \to \rho\phi$	$3.4(8) \cdot 10^{-4}$	gas.	[1]
	$4.4(12) \cdot 10^{-4}$	gas./LX	[1]
	$3.4(10) \cdot 10^{-4}$	$^1S_0$	[1]
	$3.7(9) \cdot 10^{-4}$	^3P_J	[1]
$p\bar{p} \to \pi^+\pi^-\omega$	$6.6(6) \cdot 10^{-2}$	liq.	[30]
$p\bar{p} \to \rho\omega$	$5.4(6) \cdot 10^{-2}$	gas.	[29]
	$3.0(7) \cdot 10^{-2}$	S	[29]
	$6.4(11) \cdot 10^{-2}$	P	[29]
	$2.3(2) \cdot 10^{-2}$	liq.	[30]
$p\bar{p} \to \pi^+\pi^- K_S K_L$	$2.41(36) \cdot 10^{-3}$	liq.	[36]
	$2.26(45) \cdot 10^{-3}$	liq.	[35]

resonance. The two-step mechanism $p\bar{p} \to \pi\pi K\bar{K} \to \pi\pi\phi$ was estimated as well in [16] using the unitariry approximation and neglecting the spin structure of the amplitude, the resulting branching ratio being about one order of magnitude smaller than the experimental value. In this paper we present a more detailed calculation of this mechanism which includes spin effects and off-shell contributions. It shows that $K\bar{K}$ rescattering in the $K\bar{K}\pi\pi$ system leads to a significant enhancement of the $\phi\pi\pi$ production in $p\bar{p}$ annihilation at low energies which has the right order of magnitude. Note that this straight $K\bar{K} - \phi$ rescattering mechanism cannot contribute to two body final states in the two meson doorway approximation.

3 Resonant rescattering mechanism

To illustrate the basic features of the resonant rescattering mechanism we consider a three-particle decay $a \to 123$ where particles 1 and 3 interact via resonance b. The total decay amplitude corresponds to the sum of the two diagrams shown in Figs. 1a,b. As shown in Fig. 2, all rescattering terms $1 + 2 \leftrightarrow b$ are taken into account by including the mass operator $\Pi_b(p_b^2)$ in the resonance propagator. Here and below p_n denotes the four-momentum of particle n, $p_b^2 = (p_1 + p_2)^2 = s_{12}$. The imaginary part of the mass operator $\Pi_b(s_{12})$ is determined by the width of the decay $a \to 1 + 2$:

$$\text{Im}\ \Pi_b(s_{12}) = -\sqrt{s_{12}}\Gamma_b(s_{12})\ , \tag{1}$$

$$\Gamma_b(s_{12}) = \frac{g_b^2 P_{12}(s_{12})}{8\pi s_{12}} \tag{2}$$

where g_b is the coupling constant for the decay $b \to 12$ (for the sake of illustration all particles are assumed to be spinless in this section), and $P_{12}(s_{12})$ is the three momentum of particles 1 and 2 in their CMS:

$$P_{12}(s_{12}) = \frac{1}{2}\sqrt{(s_{12} - (m_1 + m_2)^2)(1 - (m_1 - m_2)^2/s_{12})}\ . \tag{3}$$

If the resonance b is narrow, then the following approximation for the resonance propagator can be used:

$$\frac{1}{p_b^2 - m_0^2 - \Pi_b(p_b^2)} = \frac{1}{p_b^2 - m_b^2 + i m_b \Gamma_b} \tag{4}$$

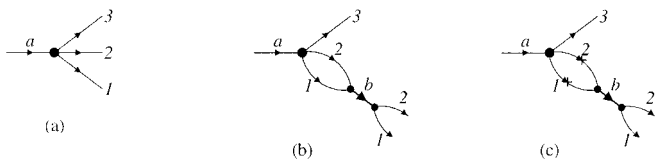

Fig. 1. **a** The amplitude $T^0_{a\to 123}$ for the decay $a \to 123$ in plane wave approximation, **b** The decay amplitude $T^{res}_{a\to 123}$ with resonant final state interaction. **c** The unitarity approximation $T^{UA}_{a\to 123}$ for the resonant FSI amplitude

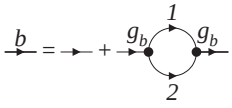

Fig. 2. The equation for the propagator of resonance b coupled to the two-particle channel $(1+2)$

where m_b and $\Gamma_b = \Gamma_b(m_b^2)$ are the physical mass and the physical width of the resonance.

The amplitude corresponding to the resonant rescattering diagram in Fig. 1b has the form

$$T^{res}_{a\to 123} = -(i+\beta(s_{12}))\frac{g_a g_b P_{12}(s_{12})}{8\pi\sqrt{s_{12}}}\frac{g_b}{s_{12}-m_b^2+im_b\Gamma_b}$$
$$= -(i+\beta(s_{12}))\frac{\sqrt{s_{12}}\Gamma_b(s_{12})}{s_{12}-m_b^2+im_b\Gamma_b} \quad (5)$$

where g_a is the coupling constant for the decay $a \to 123$, and $\beta(s_{12})$ is the ratio of the real to imaginary part of the loop in the diagram Fig. 1b. The imaginary part of the loop, which corresponds to the particles 1 and 2 on the mass shell (Fig. 1c), is determined by the coupling constant and the phase space for the decay $b \to 1+2$. The real part of the loop is divergent and must be regularized, e.g. by subtraction or by introducing form factors in the vertices:

$$g_a \to g_a F_a(s_{12}) \ , \quad (6)$$
$$g_b \to g_b F_b(s_{12}) \ . \quad (7)$$

The loop in the diagram of Fig. 1b can be calculated using the dispersion relation

$$-(i+\beta(s_{12}))\frac{P_{12}(s_{12})}{\sqrt{s_{12}}} =$$
$$= \frac{1}{\pi}\int_{(m_1+m_2)^2}^{\infty}\frac{F_a(s)F_b(s)P_{12}(s)s^{-1/2}ds}{s-s_{12}+i\epsilon} \ . \quad (8)$$

Instead of specifying the subtraction point or the form factors one can consider β as a model parameter. Neglecting the real part ($\beta = 0$) corresponds to the unitarity approximation for $T^{UA}_{a\to 123}$ for the resonant FSI amplitude (Fig. 1c).

The total amplitude $a \to 123$ has the form

$$T_{a\to 123} = g_a + T^{res}_{a\to 123} = g_a A(s_{12}) \quad (9)$$

where $A(s_{12})$ is the enhancement factor resulting from the resonant final state interaction:

$$A(s_{12}) = \left(1 - \frac{(i+\beta)m_b\Gamma_b}{s_{12}-m_b^2+im_b\Gamma_b}\right)$$
$$= \frac{s_{12}-m_b^2-2m_b\Delta}{s_{12}-m_b^2+im_b\Gamma_b} \ . \quad (10)$$

According to (9,10) the total amplitude has a pole at $s_{12} \approx (m_b - i\Gamma_b/2)^2$ and a *zero* at $s_{12} \approx (m_b+\Delta)^2$ where

$$\Delta = \beta\Gamma_b/2 \quad (11)$$

The zero of the total amplitude results from the interference between the resonant term and the nonresonant background, and it is essential for providing the correct asymptotic behaviour of the enhancement factor at large s: $A(s) \overset{s\to\pm\infty}{\longrightarrow} 1$ (see [38] and references therein).

The differential decay rate has the form

$$d\Gamma_{a\to 123} = (2\pi)^4\frac{g_a^2}{2m_a}|A((p_1+p_2)^2)|^2 \times$$
$$\times\, d\Phi_3(p_a,p_1,p_2,p_3) \quad (12)$$

where $d\Phi_3(p_a,p_1,p_2,p_3)$ is the differential 3-body phase space, see Appendix A. The distribution in the invariant mass of the pair (1+2) is given by

$$\frac{d\Gamma_{a\to 123}}{ds_{12}} = (2\pi)^7\frac{g_a^2}{2m_a}|A(s_{12})|^2\Phi_2(m_a,\sqrt{s_{12}},m_3) \times$$
$$\times\,\Phi_2(\sqrt{s_{12}},m_1,m_2) \quad (13)$$

Here and below $\Phi_n(m,m_1,\ldots,m_n)$ denotes the total n-body phase space, see Appendix A.

The resonance approximation for the production of the particles 1 and 2 corresponds to the case when only the resonant term $T^{res}_{a\to 123}$ in (9) is taken into account:

$$d\Gamma_{a\to b3\to 123} = \Gamma_{a\to b3}\,\frac{m_b\Gamma_b}{|s_{12}-m_b^2+im_b\Gamma_b|^2}\,\frac{ds_{12}}{\pi} \quad (14)$$

$$\Gamma_{a\to b3} = \int d\Gamma_{a\to b3}$$
$$= (2\pi)^7\frac{g_a^2}{2m_a}(\pi m_b\Gamma_b)(1+\beta^2) \times$$
$$\times\,\Phi_2(m_a,m_b,m_3)\Phi_2(m_b,m_1,m_2) \quad (15)$$

where $\beta = \beta(m_b^2)$. The ratio of the resonant production rate $\Gamma_{a\to b3}$ to the total rate of the decay $a \to 123$ in the plane wave approximation (without FSI)

$$\Gamma^0_{a\to 123} = (2\pi)^4\frac{g_a^2}{2m_a}\Phi_3(m_a,m_1,m_2,m_3) \quad (16)$$

is given by the formula

$$\frac{\Gamma_{a\to b3}}{\Gamma^0_{a\to 123}} = (\pi m_b\Gamma_b)(1+\beta^2) \times$$
$$\times\,\frac{(2\pi)^3\Phi_2(m_a,m_b,m_3)\Phi_2(m_b,m_1,m_2)}{\Phi_3(m_a,m_1,m_2,m_3)} \quad (17)$$
$$= (\pi m_b\Gamma_b)(1+\beta^2) \times$$
$$\times\,\frac{\Phi_2(m_a,m_b,m_3)\Phi_2(m_b,m_1,m_2)}{\int\Phi_2(m_a,m_{12},m_3)\Phi_2(m_{12},m_1,m_2)dm_{12}^2} \ .$$

Note that the off-shell contribution leads to the enhancement factor $(1+\beta^2)$. The resonance approximation (14) can be used only for $|\beta| \gg 1$, otherwise one cannot neglect the interference of the resonant term with the background. For example, if $\beta = 0$, then the peak structure arising from the resonance pole is completely suppressed by the zero

in the amplitude (9,10) at $s_{12} = m_b^2$, so that the production cross section features a dip instead of a peak in the resonance region.

The generalization to the four-particle decay $a \to 1234$ with final state interaction in the system (1+2) is straightforward. In particular, the ratio of the resonant production rate $\Gamma_{a\to b34}$ to the total rate of the decay $a \to 1234$ in the plane wave approximation is given by the formula

$$\frac{\Gamma_{a\to b34}}{\Gamma^0_{a\to 1234}} = (\pi m_b \Gamma_b)(1+\beta^2) \times \times \frac{(2\pi)^3 \Phi_3(m_a, m_b, m_3, m_4)\Phi_2(m_b, m_1, m_2)}{\Phi_4(m_a, m_1, m_2, m_3, m_4)} \quad (18)$$
$$= (\pi m_b \Gamma_b)(1+\beta^2) \times \times \frac{\Phi_3(m_a, m_b, m_3, m_4)\Phi_2(m_b, m_1, m_2)}{\int \Phi_3(m_a, m_{12}, m_3, m_4)\Phi_2(m_{12}, m_1, m_2) dm_{12}^2} .$$

The differential decay rate has the form

$$d\Gamma_{a\to 1234} = (2\pi)^4 \frac{g_a^2}{2m_a} |A((p_1+p_2)^2)|^2 \times \times d\Phi_4(p_a, p_1, p_2, p_3, p_4) . \quad (19)$$

Equations (17,18) have a very simple interpretation: the rate of resonant production is proportional to the fraction of the total phase space which overlaps with the resonant region, with the extra factor $(1+\beta^2)$ accounting for the off-mass-shell effects.

Applying (17,18) to the case of $p\bar{p}$ annihilation into $K\bar{K}\rho$ and $K\bar{K}\pi\pi$ we get the following estimates for the ϕ production:

$$\frac{\Gamma_{p\bar{p}\to\phi\rho}}{\Gamma_{p\bar{p}\to K\bar{K}\rho}} \sim (\pi m_\phi \Gamma_\phi)(1+\beta^2) \times \quad (20)$$
$$\times \frac{(2\pi)^3 \Phi_2(2m_p, m_\phi, m_\rho)\Phi_2(m_\phi, m_K, m_K)}{\Phi_3(2m_p, m_K, m_K, m_\rho)}$$
$$= 0.053(1+\beta^2) \quad (21)$$
$$\frac{\Gamma_{p\bar{p}\to\phi\pi^+\pi^-}}{\Gamma_{p\bar{p}\to K\bar{K}\pi^+\pi^-}} \sim (\pi m_\phi \Gamma_\phi)(1+\beta^2) \times$$
$$\times \frac{(2\pi)^3 \Phi_3(2m_p, m_\phi, m_\pi, m_\pi)\Phi_2(m_\phi, m_K, m_K)}{\Phi_4(2m_p, m_K, m_K, m_\rho)}$$
$$= 0.014(1+\beta^2) \quad (22)$$

Equation (22) at $\beta = 0$ agrees with the estimate given in [16].

To demonstrate the effects of resonant FSI and to explore the difference between the full loop calculation and the unitarity approximation we use the coupled channel model described in Appendix B. In this model the loop integrals are regularized by a form factor in the vertex $b \to 12$. Using a monopole form factor with cutoff parameter λ gives a ratio of the real to imaginary part of the loop $\beta = \lambda/P_{12}$. As an example we choose the masses and resonance parameters corresponding to the process $p\bar{p} \to K\bar{K}\rho$ and calculate the $\phi\rho$ final state (see below for a proper treatment of the spin factors). The results are shown in Fig. 3.

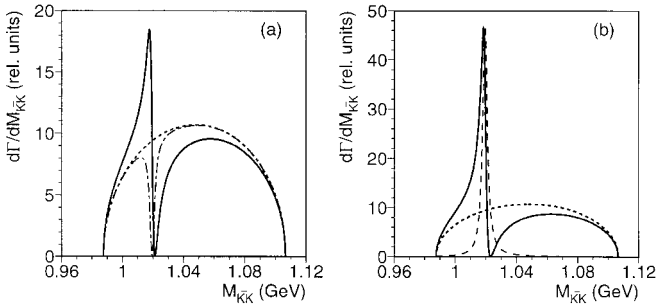

Fig. 3. The distribution of the invariant mass of the $K\bar{K}$ system for the reaction $p\bar{p} \to K\bar{K}\rho$ at rest (spinless approximation). The full rescattering calculation is given by the *solid line*: **a** $\beta = 1$, **b** $\beta = 2$, the phase space distribution by the *dotted line*. The unitarity approximation ($\beta = 0$) is shown in **a** by the *dashed-dotted line*, the resonance term in **b** by the *dashed line*. All the distributions are nomalized relatively to the total rate calculated in the plane wave approximation

4 The ϕ meson production in the reaction $\bar{p}p \to K\bar{K}\pi^+\pi^-$ at rest

In this section we consider ϕ meson production in $p\bar{p}$ annihilation at rest in the $K\bar{K}\pi\pi$ channel. The $K\bar{K}$ system must be in a P-wave with C-parity $C_{K\bar{K}} = -1$ to form the ϕ meson. The $\pi\pi$ system can be either in the C-odd or the C-even state, and, if we restrict ourselves to S-wave annihilation, the following transitions are possible:

$$J^{PC} = 1^{--} : p\bar{p}(^3S_1) \to (K\bar{K})_{L=1,P=-1,C=-1} \times (\pi\pi)_{L=even,P=+1,C=+1} \quad (23)$$
$$J^{PC} = 0^{-+} : p\bar{p}(^1S_0) \to (K\bar{K})_{L=1,P=-1,C=-1} \times (\pi\pi)_{L=odd,P=-1,C=-1} \quad (24)$$

The $p\bar{p}(^{2S+1}L_J)K\bar{K}\pi\pi$ vertices with minimum number of derivatives have the form:

$$T_{p\bar{p}(1^{--})\to K\bar{K}\pi\pi} = g_1 \epsilon_\mu^{p\bar{p}} (p_1 - p_2)^\mu F_1 \quad (25)$$
$$T_{p\bar{p}(0^{-+})\to K\bar{K}\pi\pi} = g_0 \varepsilon_{\alpha\beta\gamma\delta} p_1^\alpha p_2^\beta p_3^\gamma p_4^\delta F_0 \quad (26)$$

where g_0 and g_1 are the corresponding coupling constants, $\epsilon_\mu^{p\bar{p}}$ is the polarization vector of the $p\bar{p}(^3S_1)$ state, the p_i are the four-momenta of the particles in the final state (p_1 and p_2 correspond to K and $\bar{K}$, and p_3, p_4 to $\pi\pi$, respectively). The vertex form factors are denoted by F_1 and F_0. In the case (26), the strong $\pi\pi$ interaction due to the ρ meson must be taken into account, using e.g. the method described in Sect. 3. The results for the $p\bar{p}$ annihilation into the $\phi\rho$ channel will be published elsewhere.

In the rest of this paper we focus our attention on the ϕ production from the triplet S-wave $p\bar{p}$ state. The recent partial wave analysis of the $\phi\pi\pi$ channel measured by OBELIX [6,37] demonstrates that the S-wave reaction is dominated by the $^3S_1$ initial state if the $\pi\pi$ system is produced with invariant mass below the ρ resonance, therefore our calculations can be directly compared with

these data[2]. The coupling (25) is proportional to the relative momentum of the $K\bar{K}$ pair, $P_{K\bar{K}} = \sqrt{(p_K - p_{\bar{K}})^2}/2$, therefore the form factor in the annihilation vertex is important for damping the transition strength at large $P_{K\bar{K}}$. We use the following parametrizations:

$$F_1(P_{K\bar{K}}) = \begin{cases} \dfrac{\Lambda^2}{\Lambda^2 + P_{K\bar{K}}^2} & \text{(a) — monopole} \\ \dfrac{\Lambda^4}{(\Lambda^2 + P_{K\bar{K}}^2)^2} & \text{(b) — dipole} \end{cases} \quad (27)$$

where Λ is a cut-off parameter which will be determined later. We neglect the final $\pi\pi$ interaction in the S-wave, since the energy dependence of the FSI effects below the $f_0(980)$ resonance is known to be rather smooth (see [38] and references therein). For the sake of simplicity we also neglect the FSI effects in the $K\pi$ systems; this assumption, however, should be removed in further studies, because the K^* production is rather strong in the $K\bar{K}\pi\pi$ channel [35, 36].

The calculation of the resonant rescattering amplitude is similar to Sect.3. The result for the differential decay rate is

$$\frac{d\Gamma_{K\bar{K}\pi^+\pi^-}}{dm^2_{K\bar{K}}} = (2\pi)^7 \frac{g_1^2}{2m_{p\bar{p}}} |A_1(m^2_{K\bar{K}})|^2 \times \times W(m_{p\bar{p}}, m_{K\bar{K}}) \,, \quad (28)$$

$$W(m_{p\bar{p}}, m_{K\bar{K}}) = \Phi_3(m_{p\bar{p}}, m_{K\bar{K}}, m_\pi, m_\pi) \times \times \Phi_2(m_{K\bar{K}}, m_K, m_{\bar{K}}) \quad (29)$$

where $m_{p\bar{p}} = 2m_p$, $m_{K\bar{K}} = \sqrt{s_{K\bar{K}}} = 2\sqrt{m_K^2 + P_{K\bar{K}}^2}$ is the invariant mass of the $K\bar{K}$ system, and the enhancement factor A_1 has the form

$$A_1(s_{K\bar{K}}) = f_1(s_{K\bar{K}}) - f_1(m_\phi^2) \times \times \frac{(i + \beta(s_{K\bar{K}}))m_\phi \Gamma_\phi}{s_{K\bar{K}} - m_\phi^2 + i m_\phi \Gamma_\phi} \,, \quad (30)$$

$$f_1(s_{K\bar{K}}) = 2P_{K\bar{K}} F_1(P_{K\bar{K}}) \,. \quad (31)$$

Keeping the resonance term only gives the production rate

$$\Gamma_{\phi\pi^+\pi^-} = (2\pi)^7 \frac{g_1^2}{2\sqrt{s}} (\pi m_b \Gamma_b)(1 + \beta(s_{K\bar{K}})^2) \times \times f_1(m_\phi^2) W(m_{p\bar{p}}, m_{K\bar{K}}) \quad (32)$$

which can be compared with the total decay rate to the $K\bar{K}\pi^+\pi^-$ channel in the plane wave approximation:

$$\frac{\Gamma_{\phi\pi^+\pi^-}}{\Gamma^0_{K\bar{K}\pi^+\pi^-}} = (\pi m_b \Gamma_b)(1 + \beta^2) \times \times \frac{f_1(m_\phi^2) W(m_{p\bar{p}}, m_\phi)}{\int f_1(m^2_{K\bar{K}}) W(m_{p\bar{p}}, m_{K\bar{K}}) dm^2_{K\bar{K}}} \quad (33)$$

[2] Due to low acceptance of the $\phi\rho$ channel the yields of the $\phi\pi^+\pi^-$ channel measured by OBELIX are lower than those measured by other groups (see Table 2)

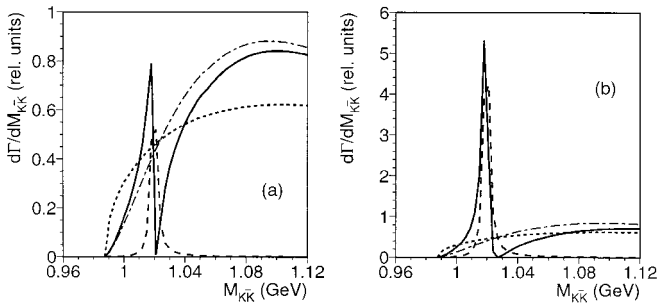

Fig. 4. The distribution of the invariant mass $m_{K\bar{K}}$ for the reaction $\bar{p}p(^3S_1) \to K\bar{K}\pi^+\pi^-$: **a** $\beta = 1$, **b** $\beta = 4$. The full calculation is given by the *solid line*, the resonance term only by the *dashed line*, the plane wave approximation by the *dash-dotted line*, the phase space distribution by the *dotted line*

For an explicit evaluation we proceed by the following steps. First, the form factor (27) is parametrized by fitting the experimental invariant mass distribution $d\sigma/dm_{K\bar{K}}$ in the mass range outside the ϕ resonance for the reaction $p\bar{p} \to (K\bar{K})_{L=1}\pi\pi$ at rest. We use the data on the reaction $p\bar{p} \to K_S K_L \pi^+\pi^-$ [36] which selects the final states $K^0\bar{K}^0$ with $C_{K\bar{K}} = -1$ and $L_{K\bar{K}} = 1$. Since the partial wave analysis for the final state $K_S K_L \pi\pi$ is not available, we must rely on some assumptions about the final state decomposition. One of them is the dominance of the S-wave annihilation, which allows two possibilities: $p\bar{p}(^3S_1, 1^{--}) \to (K^0\bar{K}^0)_{C=-1}(\pi\pi)_{C=+1}$ and $p\bar{p}(^1S_0, 0^{-+}) \to (K^0\bar{K}^0)_{C=-1}(\pi\pi)_{C=-1}$. Second, we assume that the contribution from the singlet spin state does not bring a significant distortion of the shape of $d\sigma/dm_{K\bar{K}}$ outside the ϕ meson region. The resulting cut-off parameter is $\Lambda = 0.2$ GeV for the monopole form factor (27a) and $\Lambda = 0.4$ GeV for the dipole form factor (27b).

After fixing the form factor for the $p\bar{p}$ annihilation vertex, the only parameter which remains to be determined is the ratio of the real to imaginary part, β. For the dipole form factor (27b) in the annihilation vertex, the loop in the diagram Fig. 1b is finite, and using (8) one gets

$$\beta(s_{K\bar{K}}) = \frac{3\Lambda P^2_{K\bar{K}} + \Lambda^3}{2P^3_{K\bar{K}}}, \quad (34)$$

leading to $\beta = 20$ for $\Lambda = 0.4$ GeV. If the monopole form factor (27a) is used in the annihilation vertex, then an additional form factor is needed for the ϕKK vertex. Introducing a monopole form factor with the cutoff parameter $\Lambda_\phi = \Lambda$ leads again to (34), and $\beta = 4.3$ at $\Lambda = 0.2$ GeV. These estimates show that the real part of the loop is significant even for rather soft form factors because the imaginary part is suppressed by the factor $P^3_{K\bar{K}}$ corresponding to the P-wave of the relative motion in the $K\bar{K}$ system.

The results for the distribution in the invariant mass of the $K\bar{K}$ system are shown in Fig. 4 for various values of β. As already discussed in Sect. 3, the resonant FSI mechanism causes a characteristic peak-dip structrure in the invariant mass distribution around the ϕ mass. This

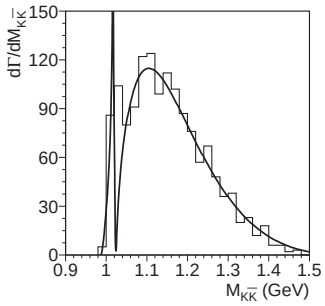

Fig. 5. The calculated distribution of the invariant mass $m_{K\bar{K}}$ for the reaction $\bar{p}p(^3S_1) \to K\bar{K}\pi^+\pi^-$ ($\beta = 2$) in comparison with the experimental data [36]

Table 3. The calculated ratio of the ϕ resonance peak to the total yield for the reaction $p\bar{p}(^3S_1) \to (K\bar{K})_{L=1}(\pi\pi)_{L=0}$ at rest for various values of β, (5)

β	1.0	2.0	3.0	4.0
dipole form factor	0.046	0.083	0.139	0.211
monopole form factor	0.059	0.105	0.173	0.261

feature can be used to distinguish the resonant FSI mechanism from other mechanisms of ϕ production, including the intrinsic strangeness [10,11] and the two-meson doorway mechanism $p\bar{p} \to \rho\omega \to \phi\pi\pi$ [16], which give only a peak in the region of the ϕ meson. The calculated mass distribution for $\beta = 2$ is compared with the experimental data in Fig. 5. A lower limit for β can, in principle, be obtained from the experimental data using (11) provided the position of the zero is known. This requires the separation of different partial waves in the distribution of the effective mass of the $K\bar{K}$ system, which is not presently available. However, from the fact that the resonance peak in the experiment [6,37] is observed very close to the ϕ mass, i.e. its position is not shifted due to a nearby zero, we can conclude that $\beta \geq 2$. Thus both theoretical estimates and the data indicate a large value of the real part of the loop. The calculated ratio of the ϕ resonance peak to the total rate of the $(K\bar{K})_{L=1}(\pi\pi)_{L=0}$ channel is shown in Table 3 (the peak contribution is defined as the integral from the $K\bar{K}$ threshold to the zero of the production amplitude, see Figs. 4,5).

To calculate the absolute yield of the $\phi\pi\pi$ we use the measured branching ratio $BR(p\bar{p} \to K_S K_L \pi^+\pi^-) = 2.4 \cdot 10^{-3}$ [36] assuming a fraction of 3/4 for to the annihilation from the $^3S_1$ state. Considering all charge channels in the intermediate state doubles the branching ratio leading to our estimate $BR(p\bar{p} \to (K\bar{K})_{L=1}\pi^+\pi^-) = 3.6 \cdot 10^{-3}$. Using the results for the relative yield of the ϕ meson from Table 3 gives the absolute yield to the $\phi\pi^+\pi^-$ channel for the $p\bar{p}$ annihilation at rest as $BR(p\bar{p}(^3S_1) \to \phi\pi^+\pi^-) \geq 3{\cdot}10^{-4}$ for $\beta \geq 2$. This result agrees well with the OBELIX result for the $\phi\pi\pi$ yield in liquid $BR(\phi\pi^+\pi^-) = 3.5(4) \cdot 10^{-4}$ [6] (this value practically excludes the contribution from the $\phi\rho$ channel). The other measurements of $BR(\phi\pi^+\pi^-)$ shown in Table 2 give slightly higher values due to the $\phi\rho$ contribution. The ASTERIX analysis [1] gives $BR(p\bar{p}(S) \to \phi\pi^+\pi^-) = 4.7(11) \cdot 10^{-4}$ and $BR(p\bar{p}(^1S_0) \to \phi\rho) = 3.4(10) \cdot 10^{-4}$. Using these branching ratios and the fact that the singlet S-wave corresponds to about one quarter of the total annihilation in liquid one gets $BR(p\bar{p}(^3S_1) \to \phi\pi^+\pi^-) = BR(p\bar{p}(S) \to \phi\pi^+\pi^-) - \frac{1}{4}BR(p\bar{p}(^1S_0) \to \phi\rho) = 3.8(13) \cdot 10^{-4}$, in agreement with the OBELIX measurement as well as with our calculations. Note, that the old bubble chamber measurement [36] $BR(p\bar{p}(S) \to \phi_{\to K_S K_L}\pi^+\pi^-) = 1.8(3) \cdot 10^{-4}$ gives $BR(p\bar{p}(S) \to \phi\pi^+\pi^-) = BR(p\bar{p}(S) \to K_S K_L \pi^+\pi^-)/BR(\phi \to K_S K_L) = 5.4(9) \cdot 10^{-4}$ in good agreement with the LEAR results.

The two-step mechanism considered is one of many possible two-step processes. Other four-particle intermediate states to be discussed include the $K^*\bar{K}\pi\pi$, $K\bar{K}^*\pi\pi$, and $K^*\bar{K}^*\pi\pi$ states which arguably can lead to Lipkin cancelations [13]. However, because the branching ratio for these channels is much smaller than for the $K\bar{K}\pi\pi$ channel and the dispersion integral (8) is saturated mainly in the low s region due to the relatively soft form factors, we do not expect strong cancellations between the contributions from these additional four-particle states. We do not include the $\phi - \omega$ mixing term in order to avoid possible double counting[3].

The contribution of the $\rho\omega$ intermediate state, which is potentially significant [16], remains to be calculated, but there is no reason to expect that there is a cancelation between the $\rho\omega$ and $K\bar{K}\pi\pi$ terms (their relative phase is an unknown parameter).

Using (28) one can estimate the dependence of the relative $\phi\pi\pi$ yield on the invariant mass of the $p\bar{p}$. For the sake of simplicity we use the phase space distribution for the $\pi\pi$ pair and the form factors for the $(K\bar{K})_{L=1}$ system described above. The results shown in Table 4 demonstrate that the fraction of the total phase space of the $K\bar{K}\pi\pi$ system, which is favourable for the resonant ϕ production, decreases with increasing total energy. This is in qualitative agreement with the general trend seen in OZI rule violation in $p\bar{p}$ annihilation[4].

5 Conclusion

We have developed a general formalism describing resonant final state interaction in a multiparticle system. This mechanism is shown to play an important role in nucleon-antinucleon annihilation into OZI-rule breaking channels ($\phi\pi\pi$, $\phi\rho$). The resonant rescattering mechanism

[3] The $\phi - \omega$ mixing goes via a two-step mechanism with the $K\bar{K}$, $K^*\bar{K}$, $K\bar{K}^*$, $K^*\bar{K}^*$ intermediate states

[4] To obtain the absolute branching ratio for the $\phi\pi\pi$ channel from the results shown in Table 4, the energy dependence of the vertex $p\bar{p} \to (K\bar{K})_{L=1}\pi\pi$, which is experimentally unknown, must be taken into account. Because the K and $\bar{K}$ share the same s-quark line, the $K\bar{K}$ pairs are predominantly produced with limited relative orbital momentum, and the energy dependence of the relative P-wave $K\bar{K}$ production is not expected to be strong

Table 4. The calculated ratio of the ϕ resonance peak to the total yield $BR(\phi\pi\pi)/BR((K\bar{K})_{L=1}\pi\pi)$ for the reaction $p\bar{p} \to (K\bar{K})_{L=1}\pi\pi$ as a function of the total energy

$\sqrt{s_{p\bar{p}}}/m_p$	2	2.5	3	4
dipole form factor, $\beta = 2$	0.083	0.050	0.039	0.031
monopole form factors, $\beta = 2$	0.105	0.058	0.041	0.027

$\bar{p}p \to \pi^+\pi^- K\bar{K} \to \pi^+\pi^-\phi$ is studied in detail. Off-mass-shell contributions are found to be very significant for this process, while the unitarity approximation is small. The interference of the resonant term with the nonresonant background which is essential for providing a correct analytical structure of the total amplitude in the case of elastic resonant rescattering, leads to the characteristic peak-dip structure of the invariant $K\bar{K}$ mass distribution for $J^P_{K\bar{K}} = 1^-$. This feature can help to distinguish the resonant FSI mechanism from other mechanisms of ϕ production when high resolution partial wave analysis of the $K\bar{K}$ production becomes available. The ϕ peak can get an additional enhancement due to this interference effect. The rate of the $\phi\pi\pi$ production at rest from the $^3S_1$ state is in good agreement with the experimental data [1,6,30]. Thus no unexplained OZI rule violation is required in this case — the same conclusion was obtained earlier for the $\phi\pi^0$, $\phi\phi$, $\phi\gamma$ channels as well (see [24,26,27] and references therein). The ϕ production due to resonant FSI decreases with increasing total energy as the fraction of the total phase space favourable for the resonance formation gets smaller. This feature agrees with the general trend of the OZI rule violation in the nucleon-antinucleon annihilation which is decreasing as a function of energy.

It would be desirable to extend the present approach to the case when resonant FSI effects are taken into account simultaneously in the different subsystems mentioned earlier in order to achieve a unified description of the production of the ϕ, ρ, and K^* resonances.

We are grateful to M. Sapozhnikov and B.-S. Zou for stimulating discussions.

A Appendix: Phase space

The differential n-particle phase space $d\Phi_n(p, p_1, p_2, \ldots, p_n)$ is defined by

$$d\Phi_n(p, p_1, p_2, \ldots, p_n) = \\ = (2\pi)^{-3n}\delta^4(p - \sum_{i=1}^{n} p_i)\prod_{i=1}^{n}\frac{d^3\mathbf{p}_i}{2E_i} \quad (35)$$

where p is the total four-momentum of the particles with four-momenta $p_i = (E_i, \mathbf{p}_i)$. The phase space reduction formula has the form

$$d\Phi_n(p, p_1, p_2, \ldots, p_n) = d\Phi_{n-1}(p, p_x, p_3, \ldots, p_n) \times \\ \times d\Phi_2(p_x, p_1, p_2)(2\pi)^3 dp_x^2 \quad (36)$$

The total n-particle phase space for the decay $a \to 12\ldots n$ is

$$\Phi_n(m_a, m_1, m_2, \ldots, m_n) = \int d\Phi_n(p, p_1, p_2, \ldots, p_n)\,, \\ p^2 = m_a^2\ . \quad (37)$$

B Appendix: Resonant FSI in a coupled channel model

In order to describe the resonant final state interaction in a two-particle system, we introduce a variant of the Weisskopf-Wigner (WW) model with two channels. Channel 1 is the scattering channel of interest, and channel 2 has a bound state $|b\rangle$ with bare mass m_0^2 (the rest of the dynamics in the second channel is ignored). The only interaction in the model results from the coupling between the channels. The T-matrix, as a function of the invariant mass squared s, is defined by the Lippmann-Schwinger equation

$$\begin{pmatrix} T_{11} & T_{12} \\ T_{21} & T_{22} \end{pmatrix} = \begin{pmatrix} 0 & V \\ V^+ & 0 \end{pmatrix} + \\ + \begin{pmatrix} 0 & V \\ V^+ & 0 \end{pmatrix}\begin{pmatrix} G_1^0(s) & 0 \\ 0 & G_2^0(s) \end{pmatrix}\begin{pmatrix} T_{11} & T_{12} \\ T_{21} & T_{22} \end{pmatrix} \quad (38)$$

where V is the interaction between channels 1 and 2 and $G_1^0(s)$ and $G_1^0(s)$ are the free Green functions:

$$G_1^0(s) = \frac{2}{\pi}\int_0^\infty \frac{|k\rangle\langle k|}{s/4 - m^2 - k^2}k^2 dk \quad (39)$$

$$G_2^0(s) = \frac{|b\rangle\langle b|}{s - m_0^2}\ . \quad (40)$$

Here $|k\rangle$ denotes the free two-particle state with relative momentum k, both particles have the same mass m, and $s = 4(k^2 + m^2)$. We assume the channel coupling to have the following form (all particles are spinless)

$$\langle k|V|b\rangle = g\xi(k) = \frac{g}{k^2 + \mu^2} \quad (41)$$

where g is the coupling constant and μ characterizes the range of interaction.

The solution for the scattering amplitude in channel 1 has the form

$$f(s) = -\langle k|T_{11}(s)|k\rangle = -\frac{g^2\xi(k)^2}{s - m_0^2 - \Pi(s)} \quad (42)$$

where the mass operator $\Pi(s)$ is given by

$$\Pi(s) = g^2\langle\xi|G_1^0(s)|\xi\rangle = \frac{g^2}{2\mu(k + i\mu)^2}\ . \quad (43)$$

From (42,43) the poles of the amplitude can be easily found. For the sake of illustration we consider the case of weak coupling (the bare state b is assumed to be above the threshold of the scattering channel), then the scattering

amplitude has a resonance pole at $s = (m_b - i\Gamma_b/2)^2 \approx m_0^2 + \Pi(m_0^2)$. The resonance shift $\delta m_b = m_b - m_0$ and width Γ_b due to the coupling to the open channel have the form

$$\delta m_b \approx \frac{\mathrm{Re}\ \Pi(m_0)}{2m_0} \tag{44}$$

$$\Gamma_b \approx -\frac{\mathrm{Im}\ \Pi(m_0)}{m_0} = \frac{2g^2 k_b^2 \xi^2(k_b)}{m_0} \tag{45}$$

where $k_b = \sqrt{m_b^2/4 - m^2}$.

Now we consider the decay $a \to 123$ described by a pointlike vertex with a coupling constant g_a. Using standard results from scattering theory we find that the decay amplitude with the final state interaction between particles 1 and 2 taken into account is proportional to the scattering wave function at zero distance r_{12} between particles 1 and 2. The result for the above described model has the form

$$\begin{aligned} F_{a\to 123} &= g_a \langle r_{12}=0|k_{12}^{(+)}\rangle \\ &= g_a \langle r_{12}=0|k_{12}\rangle + \\ &\quad + \langle r_{12}=0|G_0(s_{12})T(s_{12})|k_{12}\rangle \qquad (46) \\ &= g_a \left(1 - \frac{g^2(\mu + ik_{12})\xi^2(k_{12})}{s_{12} - m_0^2 - \Pi(s_{12})}\right) \qquad (47) \end{aligned}$$

where the relative momentum k_{12} is related to the the square of the invariant mass of the subsystem (1+2):

$$s_{12} = 4(m^2 + k_{12}^2)\ . \tag{48}$$

Formula (47) can be rewritten explicitly showing the pole-zero structure of the amplitude:

$$F_{a\to 123} = g_a \frac{s_{12} - m_0^2 - \Delta(s_{12})}{s_{12} - m_0^2 - \Pi(s_{12})} \tag{49}$$

$$\Delta(s_{12}) = \frac{g^2}{2\mu}\frac{1}{(k_{12}^2 + \mu^2)}\ . \tag{50}$$

Note that the nominator in (49) is a real function for real s_{12} which has a zero at $s_{12} = m_z^2 \approx m_0^2 + \Delta(m_b^2)$. The distance between the zero and the pole in the weak coupling limit is

$$m_z - m_b = \frac{\mu\Gamma_b}{2k_b}\ . \tag{51}$$

References

1. Reifenröther, J., et al.: Phys. Lett. **B267**, 299 (1991)
2. Ableev, V.G., et al.: Phys. At. Nuclei **57**, 1716 (1994)
3. Ableev, V.G., et al.: Phys. Lett. **B334**, 237 (1994)
4. Amsler, C., et al.: Phys. Lett. **B346**, 363 (1995)
5. Bertolotto, L.. et al.: Phys. Lett. **B345**, 325 (1995)
6. Bertin, A., et al.: Phys. Lett. **B388**, 450 (1996)
7. Okubo, S.: Phys. Lett. **5**, 165 (1963)
8. Zweig, G.: CERN Preprint 8419 / TH-412 (1964)
9. Iizuka, I.: Progr. Theor. Phys. Suppl. **37**, 21 (1966)
10. Ellis, J., Gabathuler, E., Karliner, M.: Phys. Lett. **B217**, 173 (1989)
11. Ellis, J., Karliner, M., Kharzeev, D.E., Sapozhnikov, M.G.: Phys. Lett. **B353**, 319 (1995)
12. Gutsche, T., Faessler, A., Yen, G.D., Yang, S.N.: Nucl. Phys. B (Proc. Suppl.) **56A**, 311 (1997); Gutsche, T.: Talk at the workshop "The Strange Structure of the Nucleon", CERN, March 11–15, 1997
13. Lipkin, H.J.: Nucl. Phys. **B244**, 147 (1984)
14. Lu, Y., Zou, B.S., Locher, M.P.: Z. Phys. **A 345**, 207 (1993)
15. Locher, M.P., Lu, Y., Zou, B.S.: Z. Phys. **A 347**, 281 (1994)
16. Locher, M.P., Lu, Y.: Z. Phys. **A 351**, 83 (1994)
17. Buzatu, D., Lev, F.M.: Phys. Lett. **B329**, 143 (1994)
18. Buzatu, D., Lev, F.M.: JINR preprint, E4-94-158, Dubna, 1994
19. Mull, V., Holinde, K., Speth, J.: Phys. Lett. **B 334**, 295 (1994)
20. Buzatu, D., Lev, F.M.: Phys. Rev. C **51**, R2893 (1995)
21. Buzatu, D., Lev, F.M.: Phys. At. Nucl. **58**, 480 (1995)
22. Gortchakov, O., Locher, M.P., Markushin, V.E., von Rotz, S.: Z. Phys. **A 353**, 447 (1996)
23. Anisovich, A.V., Klempt, E.: Z. Phys. **A 354**, 197 (1996)
24. Locher M.P.: Proc. III Conf. on Low Energy Antiproton Physics, Bled, 1994, Eds. G. Kernel, P. Križan, M. Mikuž, World Sci., 1995, p. 38.
25. Sapozhnikov M.G.: Proc. III Conf. on Low Energy Antiproton Physics, Bled, 1994, Eds. G. Kernel, P. Križan, M. Mikuž, World Sci., 1995, p. 355.
26. Zou, B.S.: Phys. At. Nucl. **59**, 1427 (1996)
27. Markushin, V.E.: Nucl. Phys. B (Proc. Suppl.) **56A**, 303 (1997)
28. Wiedner, U.: Nucl. Phys. B (Proc. Suppl.) **56A**, 299 (1997)
29. Weidenauer, P., et al.: Phys. Lett. **B267**, 299 (1991)
30. Bizzari, R., et al.: Nucl. Phys. **B14**, 169 (1969)
31. Cooper, A.M., et al.: Nucl.Phys. **B146**, 1 (1978)
32. Donald, R.A., et al.: Phys.Lett. **B61**, 210 (1976)
33. Chen, C.K., et al.: Nucl.Phys. **B130**, 269 (1977)
34. Review of Particle Properties: Phys. Rev. D **54**, 98 (1996)
35. Armenteros, R., French, B.: Antinucleon-nucleon interaction, in *High Energy Physics, Vol.IV*, Ed. E.H.S. Burhop, Academic Press, NY, 1969, p.237.
36. Barash, N., Kirsch, L., Miller, D., Tan, T.H.: Phys. Rev. **145**, 1095 (1966)
37. Bertin, A., et al.: Phys. At. Nucl. **59**, 1450 (1996)
38. Locher, M.P., Markushin, V.E., Zheng, H.Q.: Phys. Rev. D **55**, 2894 (1997)